nature catalysis

SUPPLEMENTARY INFORMATION

https://doi.org/10.1038/s41929-019-0353-0

In the format provided by the authors and unedited.

Engineered enzymes that retain and regenerate their cofactors enable continuous-flow biocatalysis

Carol J. Hartley[1], Charlotte C. Williams[2], Judith A. Scoble[2], Quentin I. Churches[2], Andrea North[2], Nigel G. French[1], Tom Nebl[2], Greg Coia[2], Andrew C. Warden[1], Greg Simpson[3], Andrew R. Frazer[3], Chantel Nixon Jensen[4], Nicholas J. Turner[4] and Colin Scott[1]*

[1]Biotechnology and Synthetic Biology Group, CSIRO Land and Water, Black Mountain Science and Innovation Precinct, Canberra, Australia. [2]CSIRO Manufacturing, Parkville, Victoria, Australia. [3]CSIRO Manufacturing, Clayton, Victoria, Australia. [4]School of Chemistry, Manchester Institute of Biotechnology, University of Manchester, Manchester, UK. *e-mail: colin.scott@csiro.au

Supplementary Information

Engineered Enzymes that Retain and Regenerate their Cofactors Enable Continuous-Flow Biocatalysis

Carol J. Hartley[1], Charlotte C. Williams[2], Judith A. Scoble[2], Quentin I. Churches[2], Andrea North[2], Nigel G. French[1], Tom Nebl[2], Greg Coia[2], Andrew C. Warden[1], Greg Simpson[3] Andrew R. Frazer[3], Chantel Nixon Jensen[4], Nicholas J. Turner[4], Colin Scott[1].

[1]*Biotechnology and Synthetic Biology Group, CSIRO Land & Water, Black Mountain Science & Innovation Precinct, Canberra, Australia*

[2]*CSIRO Manufacturing, 343 Royal Parade, Parkville, Victoria 3052, Australia*

[3]*CSIRO Manufacturing, Bag 10, Bayview Avenue, Clayton, Victoria 3168, Australia*

[4]*School of Chemistry, Manchester Institute of Biotechnology, University of Manchester, UK*

Email: colin.scott@csiro.au

Content

Supplementary Table 1. Biochemical characterization of the individual enzymes and multi-enzyme fusions used in this study.

	Optimal Reaction pH (pH range)	T_{50}* (°C)	Oligomeric Structure	k_{cat}/K_M (s^{-1} M^{-1})	Reference
Glycerol phosphorylation					
$GlpK_{TK}$	8.0 (6.5-9.5)	> 100	Monomer	6.1×10^7	[27]; This study
$GlpK_{Tk}$-$AceK_{Ms}$		58	Dimer	7.7×10^7	This study
$GlpK_{Tk}$-$AceK_{Ms}$-$Est2_{Aa}$		59	monomer/hexamer	8.6×10^7	This study
Acetate dephosphorylation (ADP phosphorylation)					
$AceK_{Ms}$	7.4 (6.0-8.5)	52	homodimer	2.8×10^6	[28]; This study
$GlpK_{Tk}$-$AceK_{Ms}$		50	Dimer	5.4×10^5	This study
$GlpK_{Tk}$-$AceK_{Ms}$-$Est2_{Aa}$		63	monomer/hexamer	9.1×10^5	This study
Glycerol-3-phosphate oxidation					
$G3PD_{Ec}$	9.0 (8.0-9.5)	51	monomer	1.4×10^6	[18]; This study
$G3PD_{Ec}$-NOX_{Ca}		37	Dimer	1.8×10^4	This study
$G3PD_{Ec}$-NOX_{Ca}-$Est2_{Aa}$		45	Dimer	1.1×10^4	This study
Oxygen reduction (NADH oxidation)					
Nox_{Ca}	7.0 (7.0-9.0)	37	homodimer	4.9×10^6	[29]; This study
$G3PD_{Ec}$-NOX_{Ca}		37	dimer	6.2×10^6	This study
$G3PD_{Ec}$-NOX_{Ca}-$Est2_{Aa}$		37	dimer	4.6×10^6	This study
Aldol addition					
$FruA_{Sc}$	6.5-9.0	> 95	monomer	3.2×10^4	[30]
$FruA_{Sc}$-$Est2_{Aa}$		81	monomer	1.3×10^5	This study
Esterase[1]					
$Est2_{Aa}$	7.1 (5.5-8.0)	80	monomer	8.3×10^5	[31]; This study

* T_{50} the temperature at which, after 30 min of incubation, 50% of the initial enzyme activity remains. The T_{50} values are the averages of at least three independent assays. Standard deviations were below 1.0 °C in all cases. pH optima did not vary between individual and fusion enzymes.

47 **Supplementary Table 2. Expression vectors and conditions used.**

Enzyme	Plasmid	Expression Vector	Cloning sites	GenBank Accession Number	Host Cells	Induction Conditions
Phosphotransfer						
$GlpK_{TK}$	pCJH1	pETCC2	*Nde* I - *Eco* R1	MK910748	*E.coli* BL21DE3 Star	1mM IPTG; 37°C, 18h
$AceK_{Ms}$	pCJH2	pDEST17	Gateway	MK910749	*E.coli* BL21AI	20mM arabinose 15°C, 18h
$GlpK_{TK}$-$AceK_{Ms}$	pCJH3	pETCC2	*Nde* I - *Bam* HI	MK910750	*E.coli* BL21DE3 Star	1mM IPTG; 37°C, 18h
$GlpK_{TK}$-$AceK_{Ms}$-$Est2_{Aa}$	pCJH4	pETCC2	*Nde* I - *Bam* HI	MK910751	*E.coli* BL21DE3 Star	1mM IPTG; 37°C, 18h
Oxidation						
$G3PD_{Ec}$	pCJH5	pDEST17 (Invitrogen)	Gateway	MK910752	*E.coli* BL21AI	20mM arabinose 25°C, 18h
NOX_{Ca}	pCJH6	pETCC2	*Nde* I - *Eco* RI	MK910753	*E.coli* BL21DE3 Star	1mM IPTG; 37°C, 18h
$G3PD_{Ec}$-NOX_{Ca}	pCJH7	pETCC2	*Nde* I - *Bam* HI	MK910754	*E.coli* BL21DE3 Star	1mM IPTG; 25°C, 18h
$G3PD_{Ec}$-NOX_{Ca}-$Est2_{Aa}$	pCJH8	pETCC2	*Nde* I - *Bam* HI	MK910755	*E.coli* BL21DE3 Star	1mM IPTG; 25°C, 18h
Aldol addition						
$FruA_{Sc}$	pAF1	pRSET-A	*Xho* I-*Nco* I	Q07159	*E.coli* BL21DE3	1mM IPTG; 15°C, 18h
$FruA_{Sc}$-$Est2_{Aa}$	pCJH9	pETCC2	*Nde* I- *Bam* HI	MK910756	*E.coli* BL21DE3 Star	1mM IPTG; 15°C, 18h
Conjugation						
$Est2_{Aa}$	pCJH10	pETCC2	*Nde* I- *Bam* HI	MK910757	*E.coli* BL21DE3 Star	1mM IPTG; 37°C, 18h

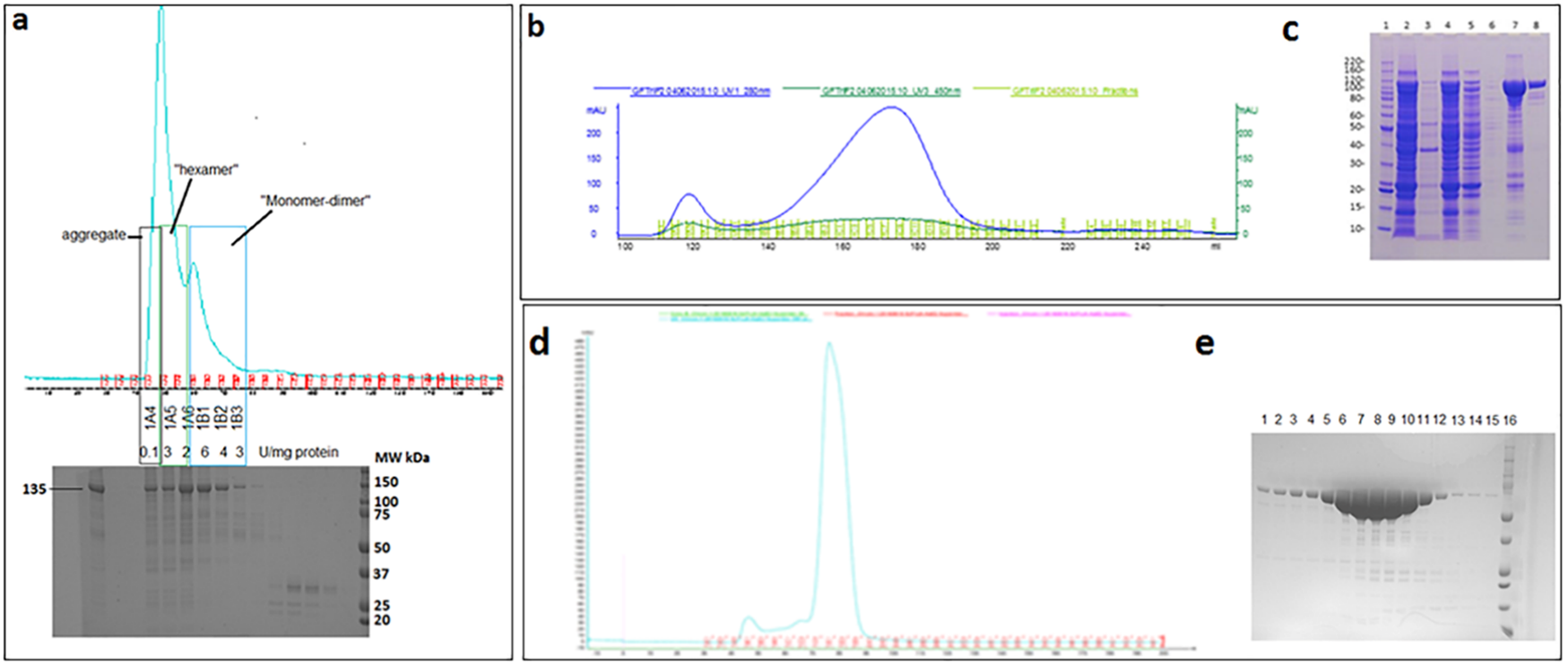

Supplementary Figure 1. Expression and purification of fusion proteins. a, Size exclusion fractionation of HIS-tag purified recombinant $GlpK_{TK}$-$AceK_{Ms}$-$E2_{Aa}$ multi-enzyme fusion protein was used to estimate oligomeric state and associated specific activity after induction with 1 mM IPTG at 15 °C for 24 h. **b,** Size exclusion fractionation of HIS-tag purified recombinant $G3PD_{Ec}$-NOX_{Ca}-$Est2_{Aa}$. Fractions from 158 – 192 mL were pooled to avoid higher MW aggregate. **c,** SDS-PAGE analysis of $G3PD_{Ec}$-NOX_{Ca}-$Est2_{Aa}$ purification. Lane 1 Benchmark™ protein molecular weight standard standard (Invitrogen), Lane 2 whole cells, Lane 3 pellet after centrifugation of lysate, Lane 4 lysate, Lane 5 HisTrap unbound, Lane 6 40 mM imidazole wash, Lane 7 300 mM imidazole elution, Lane 8 gel filtration pool. **d,** Size exclusion fractionation profile of HIS-tag purified recombinant $FruA_{Sc}$-$Est2_{Aa.}$ **e,** SDS-PAGE analysis of $FruA_{Sc}$-$Est2_{Aa}$ purification. Lane 1 Fraction 1B1, Lanes 2-15 fractions 1C1 to 2A3, Lane 16 Dual™ Protein molecular weight standard (NEB).

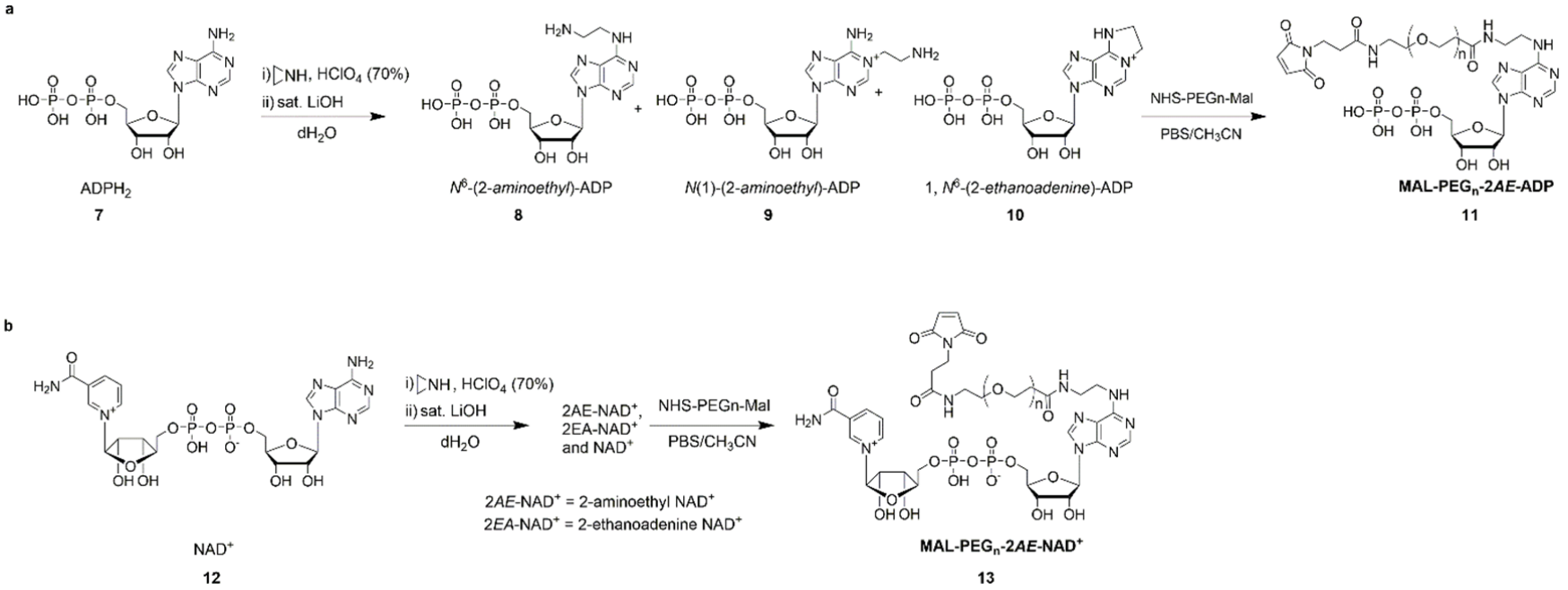

Supplementary Figure 2. Synthesis of modified cofactors for tethering to fusion proteins. **a**, Scheme for synthesis of MAL-PEG$_n$-2*AE*-ADP (**11**) from ADP (**7**). **b**, Scheme for synthetic route to prepare MAL-PEG$_n$-2*AE*-NAD$^+$ (**13**) from NAD$^+$ (**12**).

a

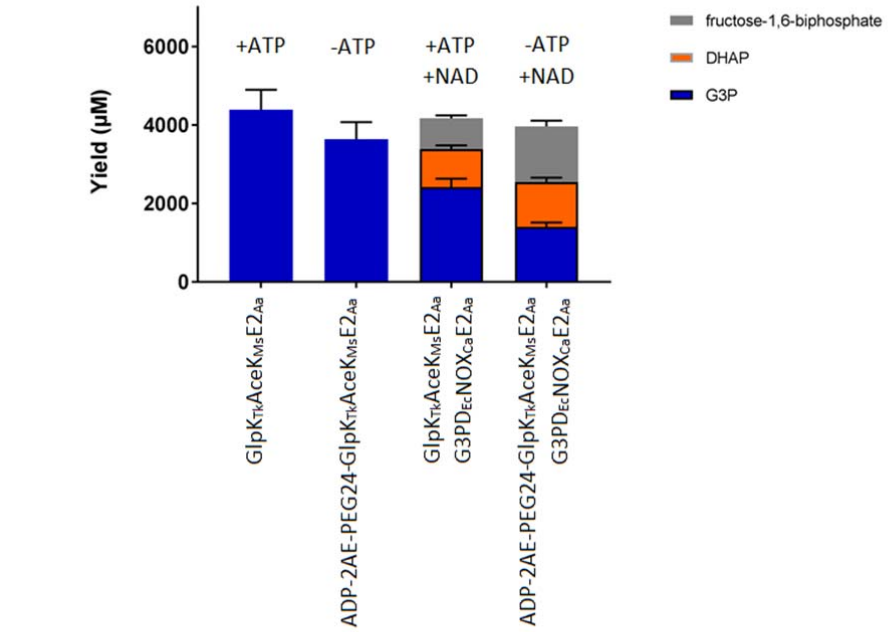
fructose-1,6-biphosphate
DHAP
G3P
Yield (µM)
6000
4000
2000
0
+ATP
-ATP
+ATP +NAD
-ATP +NAD
GlpK$_{Tk}$AceK$_{Ms}$E2$_{Aa}$
ADP-2AE-PEG24-GlpK$_{Tk}$AceK$_{Ms}$E2$_{Aa}$
GlpK$_{Tk}$AceK$_{Ms}$E2$_{Aa}$ G3PD$_{Ec}$NOX$_{Ca}$E2$_{Aa}$
ADP-2AE-PEG24-GlpK$_{Tk}$AceK$_{Ms}$E2$_{Aa}$ G3PD$_{Ec}$NOX$_{Ca}$E2$_{Aa}$

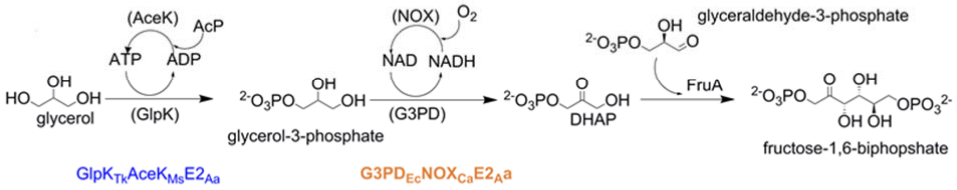
(AceK)
AcP
ATP
ADP
(GlpK)
glycerol
glycerol-3-phosphate
(NOX)
O$_2$
NAD
NADH
(G3PD)
DHAP
glyceraldehyde-3-phosphate
FruA
fructose-1,6-biphopshate
GlpK$_{Tk}$AceK$_{Ms}$E2$_{Aa}$
G3PD$_{Ec}$NOX$_{Ca}$E2$_{A}$a

b

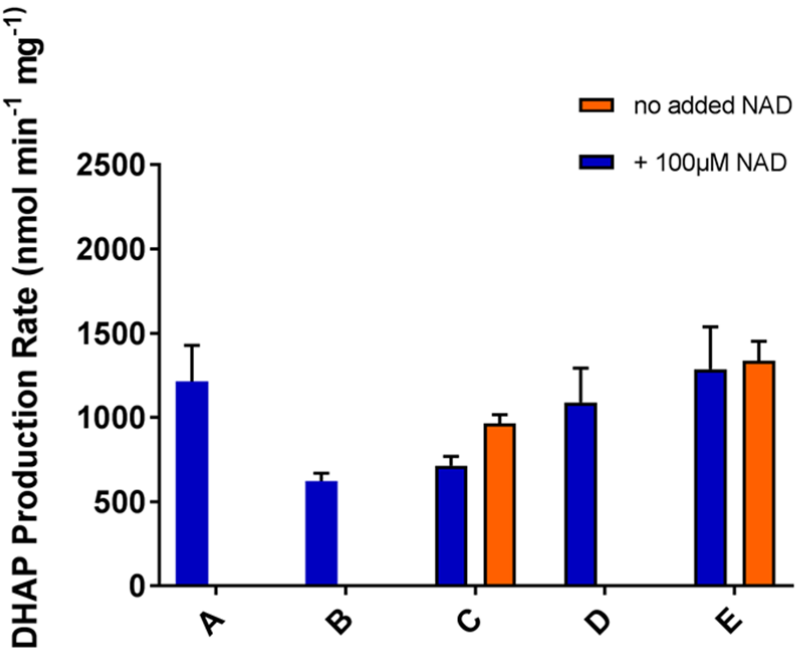
DHAP Production Rate (nmol min^{-1} mg^{-1})
2500
2000
1500
1000
500
0
no added NAD
+ 100µM NAD
A
B
C
D
E

Supplementary Figure 3. Functional tethering of modified cofactors MAL-PEG_{24}-2*AE*-ADP (a) and MAL-PEG_{24}-2*AE*-NAD^+ (b) to fusion proteins. a, Glycerolkinase activity with and without the addition of 100 µM ATP catalyzed by either 2*AE*-ADP-PEG_{24}-MAL-$GlpK_{Tk}$-$AceK_{Ms}$-$E2_{Aa}$ or by $GlpK_{Tk}$-$AceK_{Ms}$-$E2_{Aa}$ was then coupled with glycerol-3-phosphate dehydrogenase activity ($G3PD_{Ec}$-NOX_{Ca}-$E2_{Aa}$) and aldolase activity ($FruA_{Sc}$ with glyceraldehyde-3-phosphate as added donor substrate) to demonstrate the production of fructose-1,6-biphosphate from 10 mM glycerol using 2*AE*-ADP-PEG_{24}-MAL-$GlpK_{Tk}$-$AceK_{Ms}$-$E2_{Aa.}$ A scheme of the three step reaction involved is illustrated beneath the graph. **b,** Glycerol-3-phosphate dehydrogenase activity (DHAP production rate) using 10 mM glycerol-3-phosphate with and without the addition of 100 µM NAD^+ catalyzed by 2*AE*-NAD^+-PEG_{24}-MAL-$G3PD_{Ec}$-NOX_{Ca}-$E2_{Aa}$ created under different reducing and tethering conditions: untethered control $G3PD_{Ec}$-NOX_{Ca}-$E2_{Aa}$ (A), 1 mM TCEP and 1 equivalent MAL-PEG_{24}-2*AE*-NAD^+ (B), 0.1 mM TCEP and 1 equivalent MAL-PEG_{24}-2*AE*-NAD^+ (C), no TCEP and 1 equivalent MAL-PEG_{24}-2*AE*-NAD^+ (D), 1 mM TCEP and 5 equivalent MAL-PEG_{24}-2*AE*-NAD^+ (E). All reactions were conducted for 30 minutes at 37 °C, and products analysed by LCMS as described in analytical methods. Error bars indicate standard deviations from at least three independent experiments.

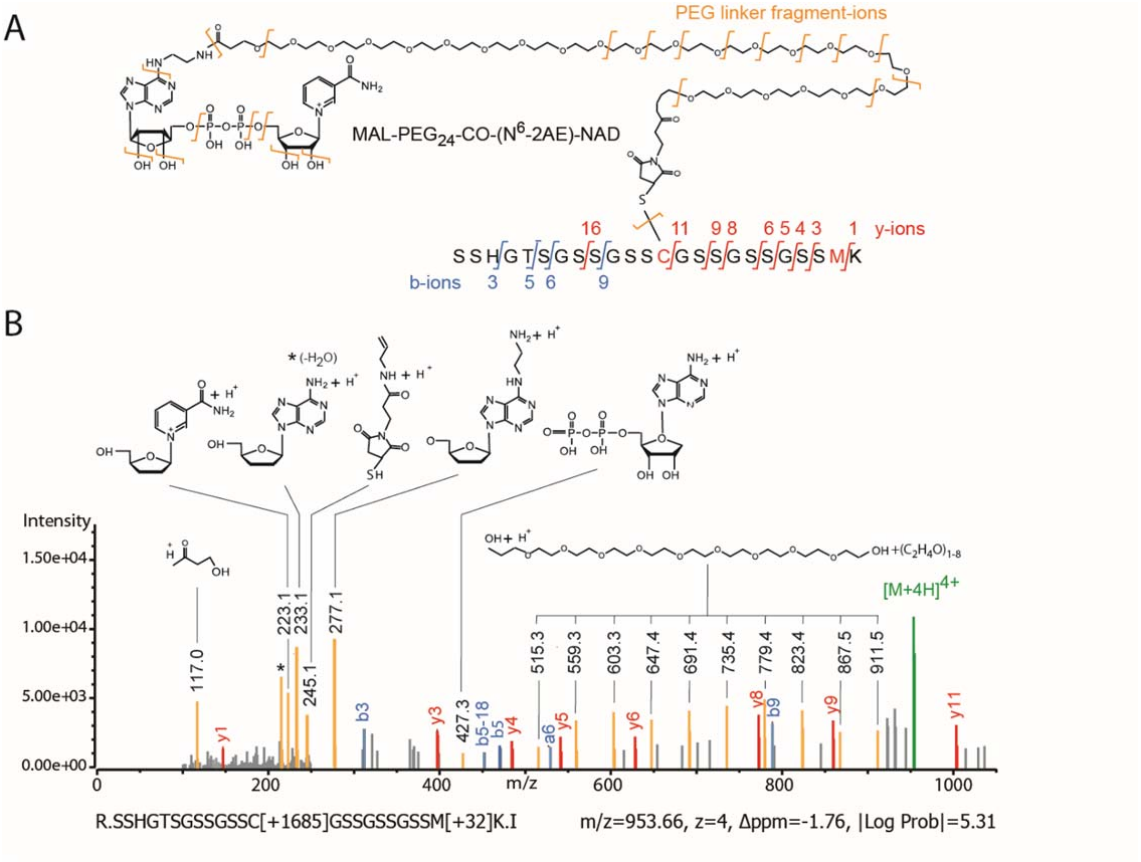

77

78 **Supplementary Figure 4: Confirmation of functional Mal-PEG$_{24}$-2*AE*-NAD$^+$ linkage to G3PD$_{Ec}$-NOX$_{Ca}$-**
79 **Est2$_{Aa}$ residue Cys369. a,** Cartoon of the chemical structure of MAL-PEG$_{24}$-2*AE*-NAD$^+$ conjugated to
80 G3PD$_{Ec}$-NOX$_{Ca}$-Est2$_{Aa}$ residue Cys369 of tryptic peptide SSHGTSGSSGSSCGSSGSSGSSMK highlighting
81 different MSMS fragment ions (peptide b-ions, blue; peptide y-ions, MAL-PEG$_{24}$-2AE-NAD$^+$ CID ions,
82 gold). **b,** Annotated LC-MSMS evidence spectrum for a high-scoring
83 R.SSHGTSGSSGSSC[+1685]GSSGSSGSSM[+32]K.I peptide highlighting peptide b- and y-ions (blue, red)
84 as well as the observed masses and chemical structures of matching MAL-PEG$_{24}$-2*AE*-NAD$^+$
85 fragments. The observed +1685Da mass modification and fragmentation pattern is consistent with
86 G3PD$_{Ec}$-NOX$_{Ca}$-Est2$_{Aa}$ Cys396 being tethered to a functional MAL-PEG$_{24}$-2*AE*-NAD$^+$ linker.

87

88

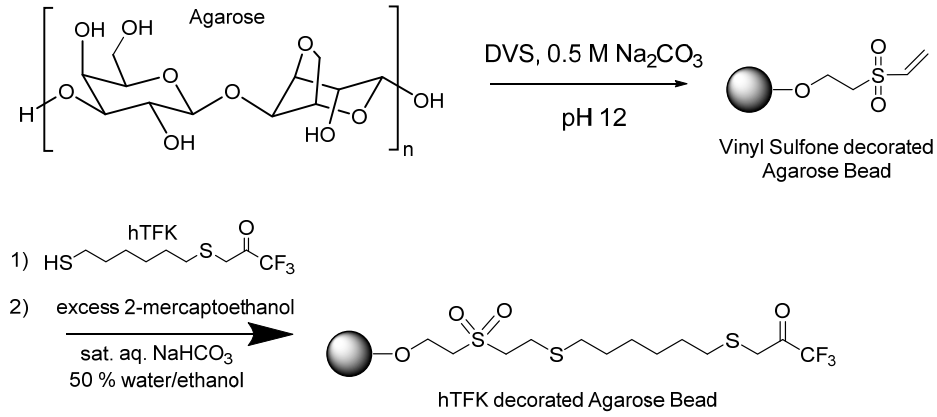

89

90

91 **Supplementary Figure 5. Scheme for the preparation of hTFK decorated agarose beads via**

92 **vinylsulfone activation.**

93

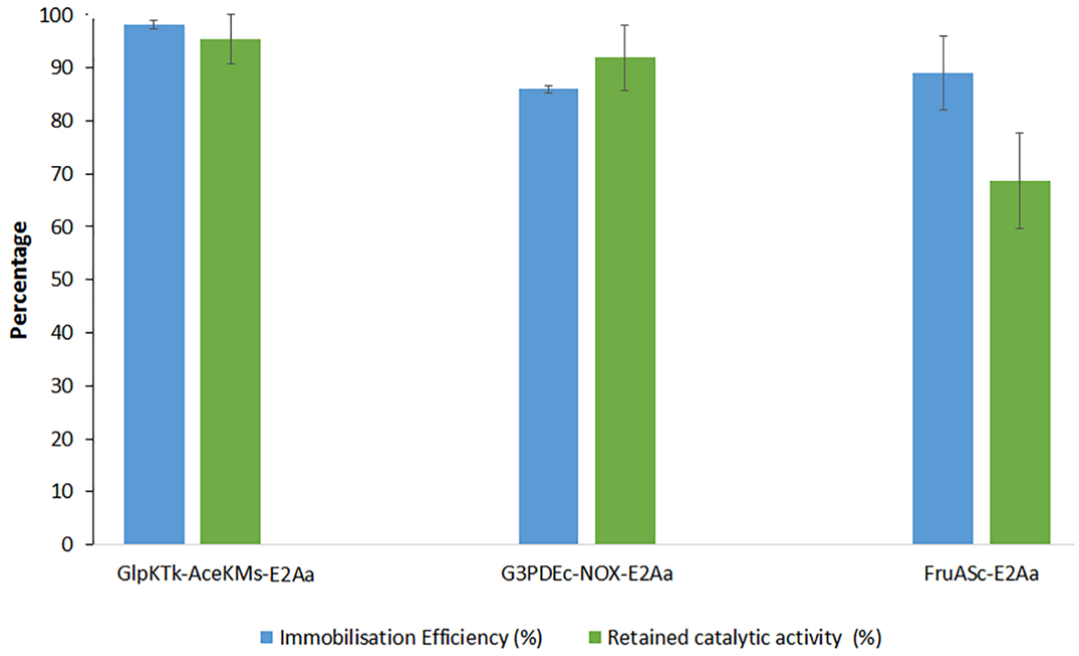

Supplementary Figure 6. Immobilisation efficiency and retention of specific catalytic activity for the fusion proteins when bound to Sepharose-DVS-hTFK beads. Error bars indicate standard deviations from at least three independent experiments

a **Phosphotransfer reactor**

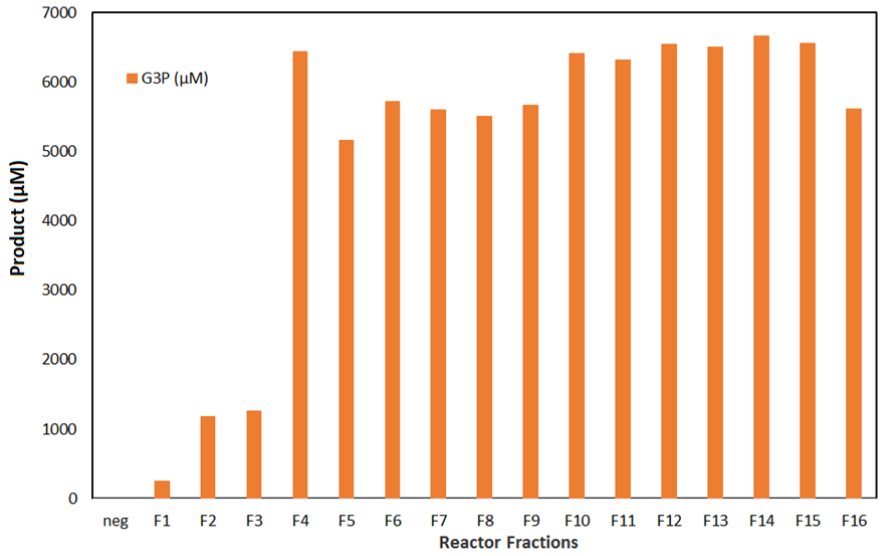

b **Oxidation reactor**

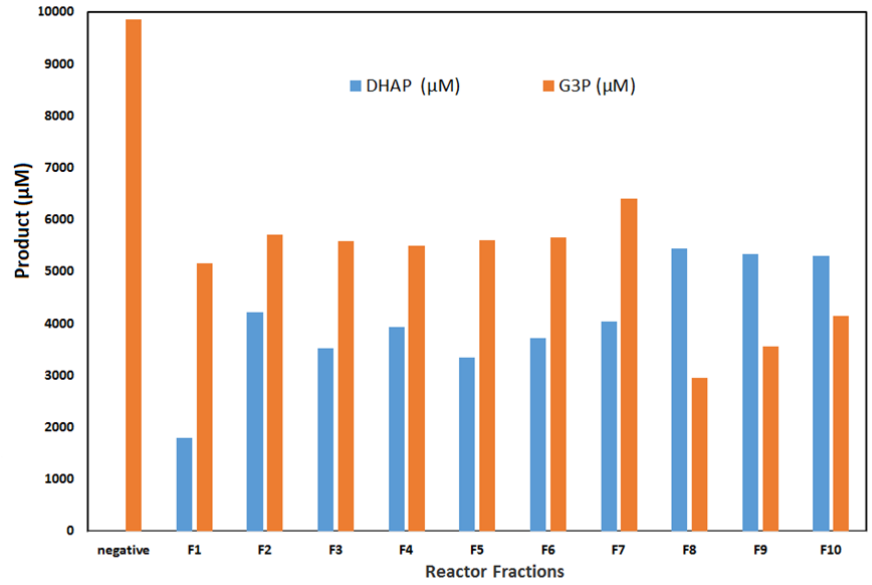

c **Aldol Addition Reactor**

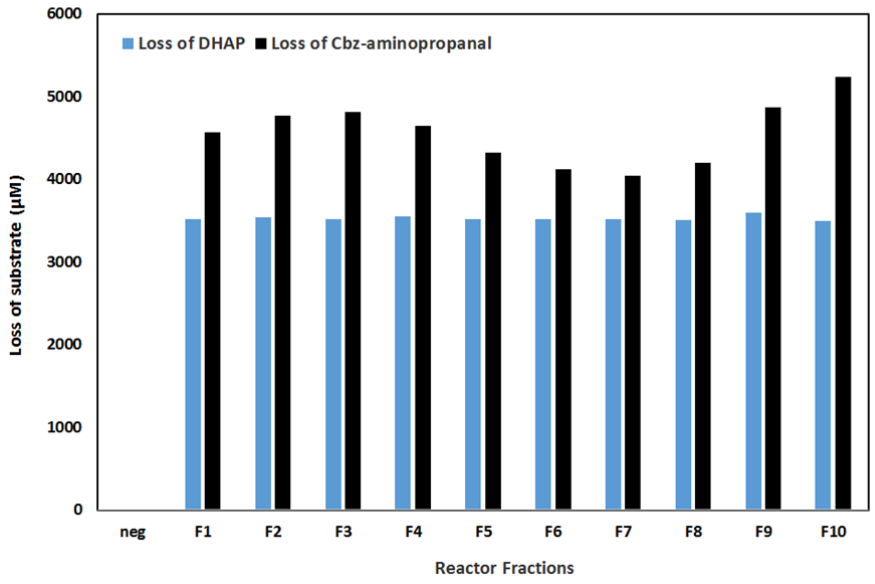

Supplementary Figure 7. Assembly and testing of each of the reactors used. a, Phosphotransfer Reactor: Conversion of glycerol and acetyl phosphate (10 mM each) to G3P and acetate by immobilized $GlpK_{Tk}$-ATP_{teth}-$AceK_{Ms}$-$Est2_{Aa}$ in a packed bed reactor column (1.5 cm id, 12 cm) run at a flow rate of 0.25 mL min^{-1}, as determined by LCMS analysis of 5 mL fractions. **b,** Oxidation reactor: conversion of G3P to DHAP in a flow reactor. The immobilized $G3PD_{Ec}$-NAD_{teth}-NOX_{Ca}-$Est2_{Aa}$ beads were used to prepare a packed bed reactor column (1.5 cm id x 16.5 cm). 10 mM G3P pH 8 was passed through the column at a flow rate of 0.25 mL min^{-1} and the amount of G3P remaining and DHAP produced determined by LCMS for 5 mL fractions F1 to F10. **c,** Aldol addition reactor with Fru_{Sc}-$E2_{Aa}$: conversion of Cbz-aldehyde and DHAP into *N*-Cbz-3*S*,4*R*-ADHOP in a flow reactor. The immobilized Fru_{Sc}-$E2_{Aa}$ beads prepared in the presence of 10 µM TCEP were used to prepare a packed bed reactor column (1.5 cm id x 16.5 cm). 5 mM *N*-Cbz-3-aminopropanal and DHAP in 50 mM citrate buffer pH 7 was passed through the column at a flow rate of 0.1 mL min^{-1} and the amount of DHAP and *N*-Cbz-3-aminopropanal remaining quantified by LCMS for 5 mL fractions F1 to F10.

a

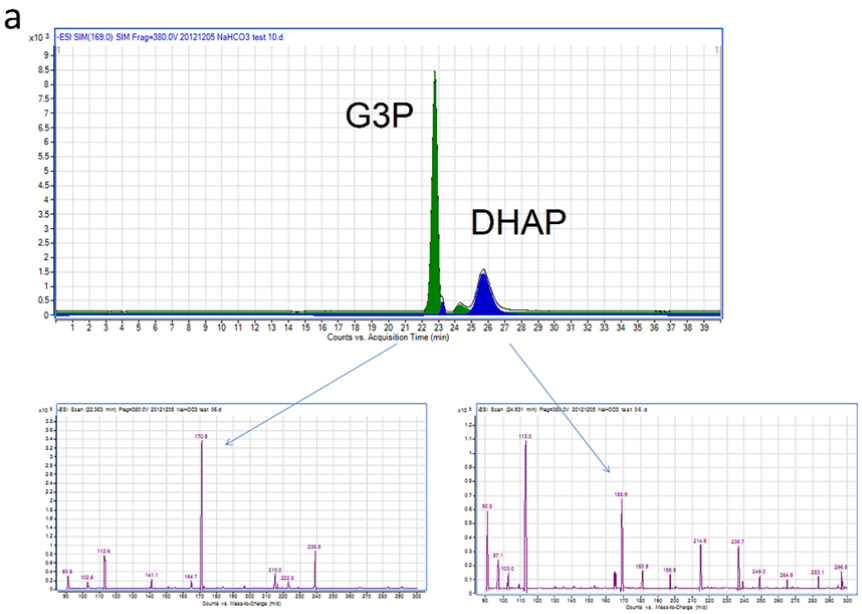
G3P
DHAP
Counts vs. Acquisition Time (min)

b

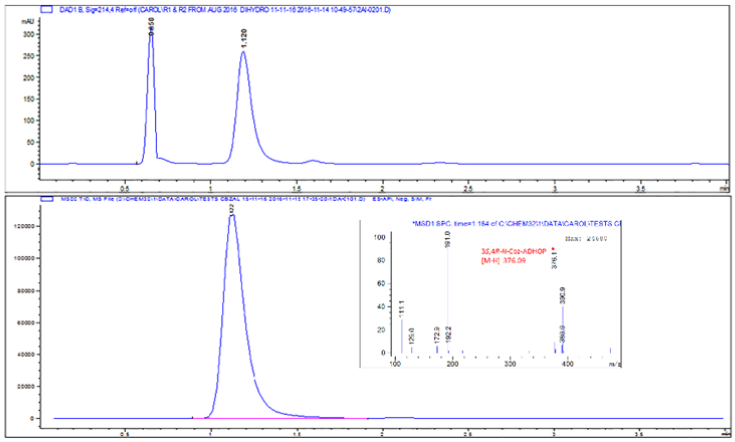

c

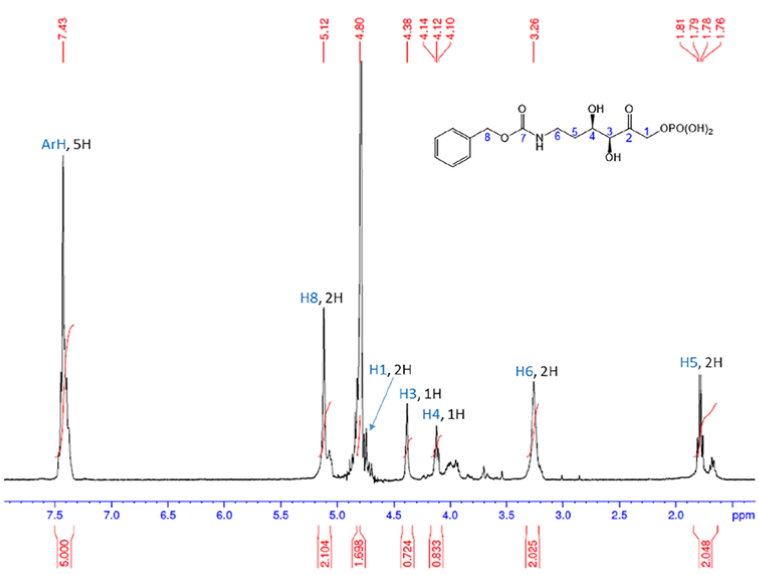
7.43
5.12
4.80
4.38
4.14
4.12
4.10
3.26
1.81
1.79
1.78
1.76
ArH, 5H
H8, 2H
H1, 2H
H3, 1H
H4, 1H
H6, 2H
H5, 2H
OPO(OH)2
ppm
5.000
2.104
1.698
0.724
0.833
2.025
2.048

117

Supplementary Figure 8. **HPLC and HPLC-MS traces and spectra for all components quantified to measure the conversion of glycerol and aldehydes into chiral aldol products. a,** HPLC separation and mass spectrometry identification of glycerol-3-phosphate (G3P) and dihydroxy acetone phosphate (DHAP). The dominant selected ions identified here (m/z 171^- for G3P and m/z 169^- for DHAP) were then used for SIM analyzes of subsequent reactions. **b,** HPLC separation of *N*-Cbz-3-aminopropanal and *N*-Cbz-3*S*,4*R*-ADHOP showing absorbance A_{214nm} (upper panel) and mass spectrometry identification of *N*-Cbz-3*S*,4*R*-ADHOP (inset). **c**, the authenticity of *N*-Cbz-3*S*,4*R*-amino-3,4-dihydroxy-2-oxyhexyl phosphate (*N*-Cbz-3*S*,4*R*-ADHOP) produced was confirmed by ^{1}H-NMR analysis of *N*-Cbz-3*S*,4*R*-ADHOP prepared by reaction of commercially available *N*-Cbz-3-aminopropanal and DHAP catalysed by FruA, and isolated by HPLC.